Electron spin resonance and electron-nuclear double-resonance investigation of a new Cr^{3+} defect on an Nb site in $LiNbO_3$:Mg:Cr

1991 J. Phys.: Condens. Matter 3 1901

(http://iopscience.iop.org/0953-8984/3/12/020)

J. Phys.: Condens. Matter 3 (1991) 1901–1908. Printed in the UK

Electron spin resonance and electron–nuclear double-resonance investigation of a new Cr^{3+} defect on an Nb site in $LiNbO_3$: Mg: Cr

G Corradi†§, H Söthe†, J-M Spaeth† and K Polgár‡

† Universität Paderborn, Fachbereich Physik, Warburger Strasse 100A, W-4790 Paderborn, Federal Republic of Germany

‡ Research Laboratory for Crystal Physics of the Hungarian Academy of Sciences, PO Box 132, H-1502 Budapest, Hungary

Received 26 November 1990

Abstract. For $LiNbO_3$ crystals heavily doped with Mg and codoped with Cr a single isotropic ESR line with $g = 1.971 \pm 0.002$ and a minimal linewidth of 1.8 ± 0.2 mT has been observed. With ENDOR it could be shown unambiguously that the new defect is Cr^{3+} substituting for Nb. The ^{53}Cr hyperfine and quadrupole constants are $A_{\parallel} = 50.8 \pm 0.2$ MHz, $A_{\perp} = 51.0 \pm 0.2$ MHz and $P = 0.10 \pm 0.05$ MHz. The crystal field at the chromium site is smaller by more than an order of magnitude than for previously reported Cr^{3+} centres in $LiNbO_3$, indicating that those centres are not on the Nb site.

1. Introduction

Electron nuclear double resonance (ENDOR) has recently proven to be most valuable in determining the positions of transition metal impurities in $LiNbO_3$ and $LiTaO_3$. Fe^{3+} ions have been found to replace Li^+ in $LiTaO_3$ (Söthe *et al* 1989) and Mn^{2+} was shown to substitute for Li^+ in $LiNbO_3$ (Corradi *et al* 1990). Up to now in Cr-doped $LiNbO_3$ similar effects prevented the location of the impurity site. As found for Cr^{3+} centres in previous ESR studies, there is an appreciable crystal field at the impurity site, resulting in an axial field constant of approximately $D = 0.4\ cm^{-1}$ (Burns *et al* 1967, Rexford *et al* 1970, Malovichko *et al* 1986). The ESR and ENDOR investigations of $LiNbO_3$ by Grachev *et al* (1987) demonstrated the propensity of Cr^{3+} to form close associates with trivalent cations such as uncontrolled Al^{3+} impurities or another Cr^{3+}, the associate presumably occupying pairs of adjacent Nb^{5+} and Li^+ sites.

In the present work, ESR and ENDOR investigations of chromium defects in $LiNbO_3$ heavily codoped with Mg have been carried out. In this system, Cr^{3+} is found to substitute for Nb. The significant differences between the previously reported and the new Cr^{3+} defect clearly suggest that different substitution sites are involved.

2. Experimental procedures

Nearly stoichiometric $LiNbO_3$ crystals were grown in air from melts having a starting

§ Present address: Research Laboratory for Crystal Physics of the Hungarian Academy of Sciences, PO Box 132, H-1502 Budapest, Hungary.

0953-8984/91/121901 + 08 $03.50

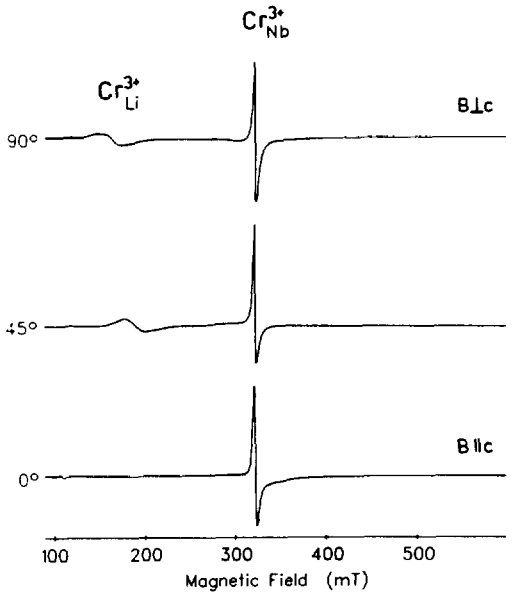

Figure 1. ESR spectra for three magnetic field orientations at $T \simeq 15$ K for $LiNbO_3$:Mg:Cr (green part of the crystal). The lines labelled Cr_{Li}^{3+} and Cr_{Nb}^{3+} are the $m_s = -\frac{1}{2} \leftrightarrow m_s = \frac{1}{2}$ transitions of Cr^{3+} on the respective substitution sites; the weak line at about 109 mT for $\boldsymbol{B} \| \boldsymbol{c}$ is the $m_s = -\frac{3}{2} \leftrightarrow m_s = \frac{3}{2}$ transition of Cr^{3+} centres.

molar Li to Nb ratio of 1:1 and doubly doped with MgO and Cr_2O_3 in concentrations of 4 mol% and 3.5×10^{-2} mol%, respectively. Merck ultrapure Li_2CO_3 and Starck Specpure Nb_2O_5 materials and a balance-controlled Czochralski growth method were used. The upper part of the boule was greenish with a continuous transition to the violet bottom part (Kovács *et al* 1988). This colour difference caused only minor intensity and linewidth variations in the ESR and ENDOR spectra.

ESR and stationary ENDOR experiments were performed with custom-built computer-controlled X-band spectrometers. The sample temperature could be varied between 10 and 300 K, the ENDOR frequency could be varied in the range between 0.5 and 300 MHz. The ENDOR line positions were determined by using digital filtering, deconvolution algorithms and a special peak search algorithm (Niklas 1983).

3. ESR spectrum

In addition to weak ESR lines of the main Cr^{3+} centre ($3d^3$ configuration, $S = \frac{3}{2}$) known from previous investigations (Rexford *et al* 1970), a single intense, essentially isotropic ESR line with $g = 1.971 \pm 0.002$ and an isotropic width was observed. The spectra for the green part of the crystal are shown in figure 1 for three orientations of the magnetic field. Here the peak-to-peak width of the new line was found to be 3.0 ± 0.3 mT. In the violet part of the crystal, where the overall concentration of Cr was found to be smaller than in the green part (Kovács *et al* 1988) and the spectrum of the previously reported Cr^{3+} could hardly be detected, the new line had a peak-to-peak width of 1.8 ± 0.2 mT. For the magnetic field parallel to the crystal axis ($\boldsymbol{B} \| \boldsymbol{c}$) the intense isotropic line overlapped the $m_s = -\frac{1}{2} \leftrightarrow m_s = \frac{1}{2}$ central transition of the previously reported Cr^{3+} centres and another weak line at about 109 mT was also observed (see figure 1), which may be due to the $m_s = -\frac{3}{2} \leftrightarrow m_s = \frac{3}{2}$ transition of the Cr^{3+} ion. Such a transition occurs at a magnetic field which is three times smaller than that of the central transition. The field positions of the mentioned Cr^{3+} transitions are independent of the crystal-field

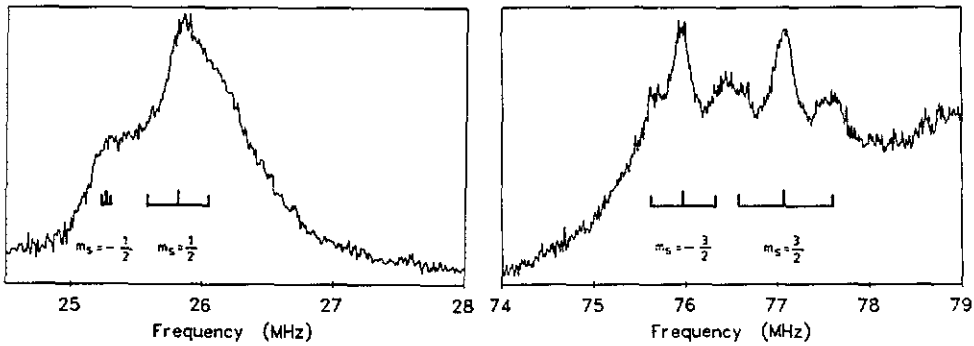

Figure 2. ^{53}Cr ENDOR spectrum for $T \simeq 10$ K and $B \| y$ measured in the centre of the isotropic ESR line at 323 mT for $LiNbO_3$:Mg:Cr (violet part). The bars indicate the positions of the ^{53}Cr quadrupole triplet lines calculated from the values given in table 1 according to equation (4).

parameter D. We cannot decide from the ESR analysis whether the weak line at about 109 mT is due to the previously reported Cr^{3+} centres or to the new centre.

4. ENDOR spectra

The ENDOR spectra consist of lines at higher frequencies due to the central nucleus and of lower-frequency transitions due to ligand nuclei. The signal-to-noise ratio and the resolution were better in the violet part of the crystal. Similarly to the case of $LiNbO_3$:Mn^{2+} (Corradi *et al* 1990) the spin-Hamiltonian

$$H = H_{Cr} + \sum H_i \tag{1}$$

$$H_{Cr} = g\mu_B \boldsymbol{B} \cdot \boldsymbol{S} + D[S_z^2 - S(S+1)/3] + A_\parallel S_z I_z + A_\perp (S_x I_x + S_y I_y) - g_n \mu_n \boldsymbol{B} \cdot \boldsymbol{I} + P[I_z^2 - I(I+1)/3] \tag{2}$$

$$H_i = \boldsymbol{S} \cdot \boldsymbol{A}_i \boldsymbol{I}_i - g_{n,i} \mu_n \boldsymbol{B} \cdot \boldsymbol{I}_i \tag{3}$$

has been used to explain all spectra, where i stands for neighbouring magnetic nuclei ($z \| c$ is the threefold optical axis of the crystal). In addition to isotropic electron and nuclear Zeeman terms an axial crystal field (parameter D), hyperfine (HF) and super-hyperfine (SHF) interactions (HF splitting constants $A_\parallel$ and $A_\perp$ for chromium and SHF tensors $\mathbf{A}_i$ for ligands) and the quadrupole interaction for chromium (splitting constant P) has been taken into account.

4.1. ^{53}Cr spectra

The isotropy of the single ESR line indicates either $S = \frac{1}{2}$ or $S > \frac{1}{2}$ with $D \simeq 0$. From the ENDOR spectra, one has the proof that the new centre, similarly to the previously reported one, also has $S = \frac{3}{2}$. In fact, spectra near 25.5 and 76.5 MHz shown for $B \| y$ in figure 2 can be attributed to electron spin projections $m_s = \pm\frac{1}{2}$ and $\pm\frac{3}{2}$, respectively. The triplet structures resolved for $m_s = \pm\frac{3}{2}$, the distance between the central components of the resolved triplets and their magnetic field dependences clearly identify the ^{53}Cr nucleus

Table 1. Axial crystal-field constants and ^{53}Cr hyperfine and quadrupole splitting constants for Cr^{3+} centres in $LiNbO_3$. For the centres contributing to the background in figure 2 the parameter variations may be much larger than indicated.

System	$\|D\|$ (cm^{-1})	$A_\parallel$ (MHz)	$A_\perp$ (MHz)	P (MHz)
$LiNbO_3$:Mg:Cr	≤ 0.01	50.8 ± 0.2	51.0 ± 0.2	0.10 ± 0.05
$LiNbO_3$:Cr	0.411[a]	49.3 ± 0.1[c]	49.3 ± 0.1[c]	-0.37 ± 0.03[c]
	0.39[b]			

[a] Rexford *et al* (1970).
[b] Malovichko *et al* (1986).
[c] Grachev *et al* (1987).

($I = \frac{3}{2}$; natural abundance, 9.5%; $g_n = -0.3147$) and exclude also the ^{25}Mg nucleus ($I = \frac{5}{2}$; natural abundance, 10.0%; $g_n = -0.3422$). Accordingly the new spectra are also due to Cr^{3+}. The $m_s = \pm\frac{3}{2}$ ENDOR lines are obtained not only in the centre of the ESR line but also for magnetic fields as far as about 20 mT apart from the central line (see section 5). For the frequency of the $m_I \leftrightarrow m_I + 1$ transition the following second-order formula has been used (see, e.g., Abragam and Bleaney 1970):

$$h\nu(\theta) = |A(\theta)m_s - h\nu_n(^{53}Cr) + [m_s^2 - S(S+1)]a^2/2g\mu_B B + (2m_I + 1)[P(\theta) - m_s a^2/2g\mu_B B]| \quad (4)$$

where θ defines the direction of the magnetic field with respect to the crystal axes, $A(\theta)$ and $P(\theta)$ are the corresponding HF and quadrupole splitting constants, respectively, the modulus of $\nu_n = g_n\mu_n B/h$ is the nuclear Larmor frequency and in the second-order terms for simplicity the isotropic HF constant $a = \frac{1}{3}(A_\parallel + 2A_\perp)$ has been used. The best-fit values of $A_\parallel$, $A_\perp$ and P are given in table 1 together with literature values for previously known Cr^{3+} centres.

4.2. Ligand ENDOR spectra

A typical low-frequency ENDOR spectrum for the green part of the crystal is shown in figure 3 for $\boldsymbol{B} \| y$ (the y direction is within a y–z glide plane of the crystal (see, e.g., Räuber 1978)). The lines between 4 and 6.6 MHz were identified to be due to ^7Li nuclei on the basis of their magnetic field dependence. The angular dependence of the ENDOR line positions for rotation of the magnetic field from the c to the y direction is shown in figure 4. In general, ENDOR lines are only seen near their extremal frequency positions. The lines broadened beyond recognition for the other field orientations. For all orientations of the magnetic field, nearly exact symmetry with respect to the Larmor frequency of ^7Li is observed. The lines shown are ascribed to $m_s = \pm\frac{1}{2}$. As shown by the unchanged positions of the ENDOR lines of ^7Li shells 1 and 4 for rotations of the magnetic field perpendicular to the c axis, these shells contain nearby nuclei on the centre c axis. In the violet samples the line of remote ^7Li nuclei at $\nu_n(^7Li)$ was much stronger. In these samples also a weak broadened $m_s = \frac{3}{2}$ line could be identified, however, only for shell 3 and $\boldsymbol{B} \| x$. Between 2 and 5 MHz also some components of the quadrupole nonet of remote Nb nuclei could be seen, similarly to $LiNbO_3$:Mn^{2+}. The experimental ^7Li spectra have been analysed by diagonalizing (3) and calculating the angular dependence.

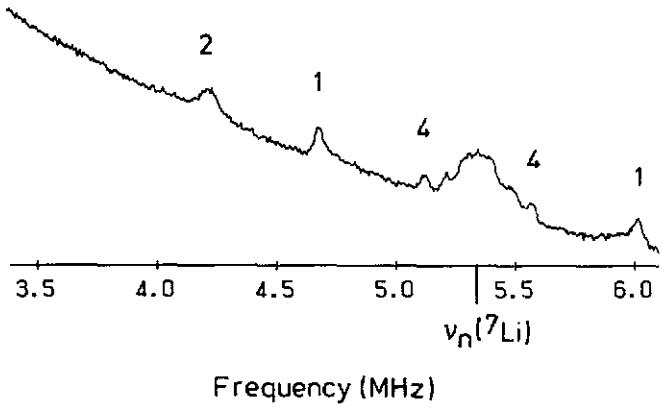

Figure 3. Part of the ^{7}Li ENDOR spectrum for $B \| y$ measured at $T = 15$ K on the isotropic ESR line at $B = 324$ mT for $LiNbO_3$:Mg:Cr (green part). The numbers above the ENDOR lines denote the ^{7}Li shell. $\nu_n(^7Li)$ is the Larmor frequency of ^{7}Li.

Table 2. Experimental and theoretical SHF parameters and polar angles defining the orientation of the third principal axes of the SHF tensors of the 'isotropic' Cr^{3+} centre in $LiNbO_3$:Mg:Cr (see text). The experimental uncertainties are 0.01 MHz and 2°, respectively. r is the distance of ligands.

	1 ^{7}Li shell 1 nucleus	2 ^{7}Li shells 3 nuclei	3 ^{7}Li shells 3 nuclei	4 ^{7}Li shells 1 nucleus
		ENDOR experiment		
a (MHz)	−0.14	0.17	0.15	0.0
b (MHz)	1.20	1.11	0.78	0.45
b' (MHz)	0	−0.03	0.01	0
ϑ (deg)	0	78	61	0
φ (deg)	—	0	0	—
		Theory: Cr^{3+} on Nb site		
r (Å)	3.063	3.067	3.357	3.870
b (MHz)	1.07	1.07	0.81	0.53
ϑ (deg)	0	76	62	0
φ (deg)	—	0	0	—

For ^{7}Li no quadrupole interactions were resolved. The results for the four nearest Li shells are given in table 2 in terms of the isotropic SHF constants a and the anisotropic SHF constants b and b', which are related to the three principal values of the SHF tensor by $A_1 = a - b + b'$, $A_2 = a - b - b'$ and $A_3 = a + 2b$. The polar angle ϑ defining the direction of the third principal axes with respect to the c axis and the polar angle φ defining their direction with respect to the y–z plane (for directions in this plane, φ = 0°) are also included. The SHF tensors are found to be essentially axial; the small values of the non-axiality parameter b' for shells 2 and 3 have been derived under the assumption that one of the principal axes is parallel to x. This is an inevitable assumption owing to the existence of y–z glide planes in $LiNbO_3$ (Corradi *et al* 1990). Random variations in the polar angles ϑ and φ may explain the strongly increased ENDOR linewidths for

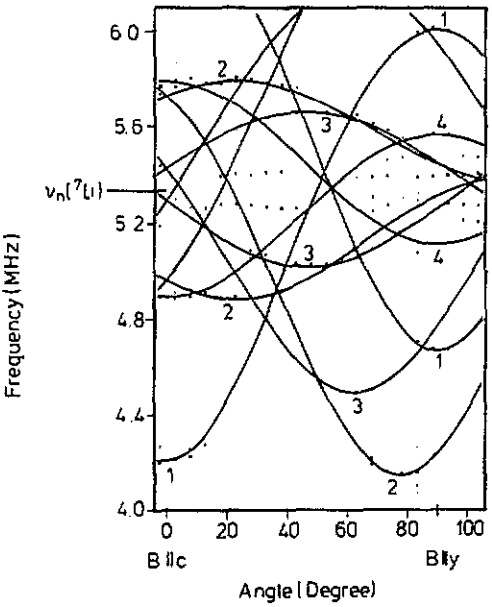

Figure 4. Experimental angular dependence of the ^{7}Li ENDOR spectrum (full circles). The full curves are calculated with the spin-Hamiltonian parameters of table 2. The numbers on the angular branches denote the Li shell responsible for the ENDOR line (see figure 5). The full circles between 5.2 and 5.5 MHz are due to distant Li neighbours.

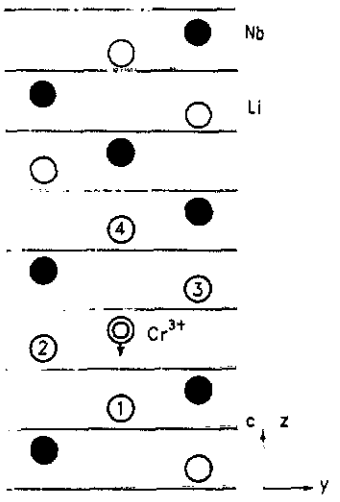

Figure 5. Identified Li shells of the Cr_{Nb}^{3+} centre in $LiNbO_3$. A small relaxation of the Cr^{3+} ion is indicated by an arrow. The horizontal lines represent oxygen planes.

general orientations of the magnetic field. The linewidths for $B \| x$ and $m_s = \frac{1}{2}$ and the orientational broadening effects are comparable with those seen for nearest Li shells of the Mn^{2+} centre in congruent $LiNbO_3$.

Assuming that the Cr^{3+} ion occupies a Nb^{5+} lattice site and calculating the anisotropic SHF interaction constants by assuming a classical point dipole–dipole interaction between the unpaired electron spin and the ^{7}Li nuclei we obtained the theoretical b-values and tensor orientations of table 2 which are in very good agreement with the experimental ones. Therefore the paramagnetic impurity must be localized at a Nb^{5+} site. For the assumption of another site in $LiNbO_3$ or for the ilmenite stacking order (Smyth 1983) the observed angular dependences cannot be explained. The applied simple point dipole approximation was found to be valid also for all Li shells in $LiTaO_3:Fe^{3+}$ (Söthe *et al* 1989) and $LiNbO_3:Mn^{2+}$ (Corradi *et al* 1990). The proposed model and the identified shells are shown in figure 5. The agreement between the experimental and calculated b-values can be further improved by assuming that the Cr^{3+} ion is closer to the 'centre' of its distorted oxygen octahedron than the lattice niobium it replaces. This relaxation may be estimated to be about 0.12 Å along the c axis, i.e. half the way from the Nb site to the location centred with respect to the x–y oxygen planes.

5. Discussion

The observed isotropy of the intense ESR line implies a rather small D-value for the axial crystal-field parameter which is not expected for $LiNbO_3$. In order to have all allowed

fine-structure split ESR transitions totally merged, D should be smaller than 5×10^{-4} cm^{-1}. This is unthinkable in $LiNbO_3$. Therefore a distribution of D leading to a broadening of the fine-structure satellites has to be considered. Assuming that $|D| \ll g\mu_B B$, for the magnetic fields $B_\parallel$ and $B_\perp$, where the $m_s = -\frac{1}{2} \leftrightarrow m_s = \frac{1}{2}$ transitions for $\boldsymbol{B} \| \boldsymbol{c}$ and $\boldsymbol{B} \perp \boldsymbol{c}$ occur, respectively, one obtains from (1) (see, e.g., Abragam and Bleaney 1970)

$$B_\perp = B_\parallel g_\parallel / g_\perp - 3D^2/4(g_\perp \mu_B)^2 B_\perp. \tag{5}$$

For a precisely isotropic g-tensor the observed isotropy and the linewidth of the ESR signal then impose a limit of $|D| < 0.01$ cm^{-1}. For some anisotropy of the g-tensor and $g_\perp < g_\parallel$, the limit may be somewhat higher. The anisotropy of g and the axial crystal-field parameter are principally interrelated and may have nearly compensating contributions to the position of the central ESR line but only for $|D| < 0.004$ cm^{-1} (see, e.g., Abragam and Bleaney 1970). These limitations allow for a linewidth of about 30 mT for the satellites even at $\boldsymbol{B} \perp \boldsymbol{c}$ which may be further increased by random non-axial crystal fields and other line-broadening mechanisms, partly active also for the central line (e.g. dipole–dipole broadening). This can make the satellites invisible. The fact that ^{53}Cr ENDOR lines for $m_s = \pm\frac{3}{2}$ can be observed as far as about 20 mT apart from the ESR line centre indicates that the fine-structure satellites are in fact smeared out and is in agreement with the estimated values of $|D|$.

Although such small D-values are unexpected in $LiNbO_3$, they may be reasonable if the Cr^{3+} ion is situated in some 'well centred' 'position in its oxygen octahedron. The Li-ENDOR analysis in fact indicates that the Cr^{3+} is displaced from the Nb site towards the location centred with respect to the x–y oxygen planes. Similar D-values have been measured for Cr^{3+} by Müller and Berlinger (1985) in all three ferroelectric phases of $BaTiO_3$ where Cr^{3+} has the same coordination. Our results confirm the conclusion of Müller and Berlinger (1985) that the Cr^{3+} ion in this coordination almost does not follow the ferroelectric displacement of the matrix cations when substituting for a cation of higher valence as Ti^{4+}, or Nb^{5+} in our case. The crystal potential experienced by the Cr^{3+} in the new centre is rather flat as shown by the small quadrupole constant in table 1. This is also in agreement with the results of Müller and Berlinger (1985). Similarly, small D-values are reported also in the pseudo-cubic crystal ScF_3 by Koryagin and Grechushnikov (1964).

Comparison of the previously reported and new Cr^{3+} centres in $LiNbO_3$ (see table 1) shows that both the crystal field and its second derivative represented by the quadrupole constant are radically different while the HF parameters are very similar. Accordingly, the Cr^{3+} ion in previously reported centres should not be on the Nb but on the Li site. (Other sites have been excluded earlier (see, e.g., Räuber 1978, Donnerberg *et al* 1989, 1990).) The change in the substitution site must be due to the massive Mg codoping. Apparently the Mg^{2+} is preferred to Cr^{3+} when substituting for Li^+ and at the same time the Mg^{2+} offers a new way for charge compensation. A similar suggestion for Fe^{3+} substitutional sites in $LiNbO_3$, undoped or doped with Mg, has been made by Feng Huixian *et al* (1990) and Böker *et al* (1990) on the basis of their ESR studies.

As shown by various line-broadening effects some disorder near the Cr^{3+} ion is strongly influencing a number of Hamiltonian parameters. Besides D and the polar angles defining the orientation of the SHF principal axes, all other interaction constants also seem to be influenced to some extent. For example the ^{53}Cr HF and quadrupole parameters may also have variations, even larger than that indicated in table 1. This is suggested by the broad background in the high-frequency ENDOR spectra (see figure 2)

and the absence of resolved ^{53}Cr HF satellites in ESR (see figure 1). Each of the latter satellites (four lines spaced at 1.8 mT) should have an integral intensity of 2.4% of the central line. The disorder may be mainly caused by the presence of charge-compensating defects at various nearby locations. Such defects may be for example Mg^{2+} ions at various Li^+ sites including also those in the nearest shells and protons associated with nearby oxygen atoms. However, neither of the two nearest Li^+ neighbours on the centre axis (i.e. the single-nucleus shells 1 and 4) may preferentially be replaced by defects since the corresponding ^7Li ENDOR lines are clearly seen. For the full compensation of a Cr^{3+} replacing Nb^{5+}, two compensators of the suggested types are needed. A Cr_{Nb}–Mg_{Li}–OH_O complex (where indices denote substitutional sites) has already been proposed by Kovács *et al* (1988) on the basis of their infrared and visible spectra obtained for the same crystal boule.

6. Conclusion

We have identified a new Cr^{3+} defect in Mg-codoped $LiNbO_3$. The Cr^{3+} ion in this defect substitutes for Nb and is slightly displaced towards a more centred position in its oxygen octahedron where it experiences a rather weak crystal field. The presence of charge compensators in the vicinity of the centre is suggested by line-broadening effects. The different properties of Cr^{3+} in the absence of Mg are attributed to Li substitution.

Acknowledgments

This work was supported by a joint project of the Deutsche Forschungsgemeinschaft (436 UNG-113) and the Hungarian Academy of Sciences, and also by the National Scientific and Research Fund of Hungary (OTKA). One of the authors (GC) gratefully acknowledges useful discussions with Professor Schirmer, Professor Földvári and Professor Michel-Calendini.

References

Abragam A and Bleaney B 1970 *Electron Paramagnetic Resonance of Transition Ions* (Oxford: Clarendon)
Böker A, Donnerberg H, Schirmer O F and Feng Xiqi 1990 *J. Phys.: Condens. Matter* **2** 6865
Burns G, O'Kane D F and Title R S 1967 *Phys. Lett.* **23** 56
Corradi G, Söthe H, Spaeth J-M and Polgár K 1990 *J. Phys.: Condens. Matter* **2** 6603
Donnerberg H, Tomlinson S M, Catlow C R A and Schirmer O F 1989 *Phys. Rev.* B **40** 11909
—— 1991 *6th Europhysical Topical Conf. on Lattice Defects in Ionic Materials (Groningen, 1990)* Abstract p 383
Feng Huixian, Wen Jinke, Wang Huafu, Han Shiying and Xu Yunxia 1990 *J. Phys. Chem. Solids* **51** 397
Grachev V G, Malovichko G I and Troitski V V 1987 *Fiz. Tverd. Tela* **29** 607 (Engl. Transl. 1987 *Sov. Phys.–Solid State* **29** 349)
Koryagin V F and Grechushnikov B N 1964 *Fiz. Tverd. Tela* **6** 422 (Engl. Transl. 1964 *Sov. Phys.–Solid State* **6** 337)
Kovács L, Földvári I, Cravero I, Polgár K and Capelletti R 1988 *Phys. Lett.* **133A** 433
Malovichko G I, Grachev V G and Lukin S N 1986 *Fiz. Tverd. Tela* **28** 991 (Engl. Transl. 1986 *Sov. Phys.–Solid State* **28** 553)
Müller K A and Berlinger W 1985 *Phys. Rev.* B **32** 5837
Niklas J R 1983 *Habilitationsschrift* Paderborn
Räuber A 1978 *Current Topics in Materials Science* vol 1, ed E Kaldis (Amsterdam: North-Holland)
Rexford D G, Kim Y M and Story H S 1970 *J. Chem. Phys.* **52** 860
Smyth D M 1983 *Ferroelectrics* **50** 93
Söthe H, Rowan L and Spaeth J-M 1989 *J. Phys.: Condens. Matter* **1** 3591